PNAS
www.pnas.org

Supporting Information for

Middle Paleolithic complex technology and a Neandertal tar-backed tool from the Dutch North Sea

Marcel J.L.Th. Niekus, Paul R.B. Kozowyk, Geeske H.J. Langejans, Dominique Ngan-Tillard, Henk van Keulen, Hans van der Plicht, Kim M. Cohen, Willy van Wingerden, Bertil van Os, Bjørn I. Smit, Luc W.S.W. Amkreutz, Lykke Johansen, Annemieke Verbaas, Gerrit L. Dusseldorp

Corresponding authors: Marcel J.L.Th. Niekus or Paul R.B. Kozowyk or Geeske H.J. Langejans

Email: marcelniekus@gmail.com or p.r.b.kozowyk@arch.leidenuniv.nl or g.langejans@tudelft.nl.

www.pnas.org/cgi/doi/10.1073/pnas.1907828 116

This PDF file includes:

Supplementary Information Text

RESULTS

Geological setting: fossiliferous content and sedimentary-architectural details

Unit B2 is a fluvial unit known to contain a considerable amount of characteristic Eemian marine and tidal-estuarine mollusk shells that were reworked from Last Interglacial deposits (1: Ockenburg Mb). Equivalent *onshore* fluvial sands are securely mapped (Fig. 2) and dated (1), resolving the Rhine-Meuse valley development during sea-level low stand in the Last Glacial in architectural relation to next older Eemian highstand and Saalian glaciation deposits. The large number of Eemian mollusk shells found at the Zandmotor (2) show the dredging for the nourishment to have reached into the zone were Unit B4 reworked Unit B2 (and may have hit in-situ portions of Unit B2 in places) (Fig. S2).

Unit B4 is a fluvial unit (wandering and braided style; larger and smaller channels (1, 3)) known to occupy a considerable width (main text) and to contain abundant and varied assemblage of terrestrial mammal bones (4). Above its basal parts, Unit B4 bar sands only contains trace quantities of (twice) reworked Eemian shells. Within Unit B4, elevated concentrations of mammal bones and gravel-sized clasts and artefacts may be found near the base of the units, but depositional niches also occur at higher levels within the unit: scour bases of shallower secondary channels, gravelly levels within bars, aggradationally preserved bar top surfaces.

We do not favor a specific depth within Unit B4 to have been the original buried position of the artefact. It is possible that approximately 50,000 years ago, it was discarded on a paleosurface marking the top of Unit B2, in which case it would be reworked and incorporated into Unit B4 shortly after. Alternatively, it is possible that it was discarded along a bar or bank of a river channel of Unit B4, at that time in the making. Dating evidence and accuracy – from radiocarbon on the artefact (this paper), and from OSL dating on Rhine sand quartz grains (1), combined and carried-over by onshore-offshore continuous geological mapping (5) – also leaves both taphonomic options open with equal weight. The radiocarbon result of c. 50,000 cal BP falls between the 1-σ OSL age-ranges (quoted from (1) supplementary materials; all from onshore part of study area in Fig. 3) for Unit B2 (87-58 ka; N=7; Median = 67 ka) and Unit B4 (30.3-48.2; N=15; Median = 37.4 ka).

THM-Pyrolysis-GC/MS

Betulin is noted and the importance of a series of long chain (di-methylated) dicarboxylic acids is demonstrated by the plot of m/z 98, a typical ion present in di-acids. Besides the typical triterpenoids betulin and lupeol, birch bark contains high amounts of suberin, a biopolymeric waxy substance (6-8). During Py-GC/MS hydrolysis and methylation

analysis, suberin in birch bark (tar) hydrolyzes into different types of long chain dicarboxylic acids and compounds, such as ferulic and coumaric acids. Subsequently, the carboxyl and hydroxyl groups of these acids and the birch bark triterpenoids, are analyzed as methyl esters and methyl ethers. Hence, the presence of a series of long chain (di-methylated) di-acids (see inset Fig. S4), together with the di-methoxylated betulin and lupeol (Fig. S4), characterize the Zandmotor material as birch bark tar.

^{14}C-AMS dating

Direct dating of a sample of the tar yielded a ^{14}C date of 47,100±500 BP (GrA-69594). The δ^{13}C value of the tar is -28.35‰, and the organic carbon content 68.5%. Both are normal values for this material (9). The date is close to the dating limit for the ^{14}C method. The measured ^{14}C activity (^{14}C/^{12}C ratio) of the tar is almost a factor 2 higher than that of the background sample, which is wood with an infinite age on the ^{14}C timescale. This demonstrates that the date presents a reliable age-estimate of the adhesive. The date obtained for the tar is just beyond the range of the IntCal13 calibration curve and hence cannot be formally calibrated (see 10). By a tentative extrapolation of the calibration curve in accordance with (11) we obtain an absolute age of approximately 50,000 calBP, placing the find in early MIS 3, a climatologically mild part within the Last Glacial (12-15). The date falls within the assemblage of OSL ages obtained for parent deposit Units B2 and B4 (median ages 67 and 37 ka respectively; Fig. S2 (1)), confirming the find's Middle Paleolithic attribution.

Techno-typological analysis of the find and optical microscopy wear analysis

The flake is made of a relatively fine-grained greyish flint. Bryozoa inclusions indicate that it is a flint from South Sweden or the southern Baltic Sea transported during the Saalian glacial (16). Valley margins of the Paleo Rhine river with Saalian gravely outwashes and deposits were located 20-25 km east and northeast of the dredging locations (17). The raw material was thus available close to the findspot (Fig. 2).

Its dimensions were measured using µ-CT scans. Technological length, from point of percussion to the distal end and following direction of percussion is 35mm. Width transversally to the axis is 30 mm (cf. 18). The maximum thickness is 11 mm. The dorsal side shows two flake scars of approximately 16 and 22 mm in length, and a natural frost-split face that was probably revealed by knapping. 40% of the dorsal surface is cortical. On the ventral side a point of impact with a cone is present; the bulb of percussion is small to medium in size with a small (~10 mm) percussion scar. The platform is plain with no preparation, and probably consists of a diaclase surface (i.e., the knapper took advantage of a naturally cracked surface to initiate the flake). The platform is 15 mm wide and 8 mm thick. The angle of percussion measures approximately 124°. At the point of impact a circular break with a diameter of ~ 4 mm is visible, indicating hard hammer percussion. Despite the presence of a few small negatives, there are no signs of extensive dorsal preparation near the platform.

Small specks of white patina are present on the flake, especially on the butt and the ventral side near the bulb of percussion. No traces of rounding were observed and the surface of the flint appears relatively fresh, except for some slight irregular 'nibbling' along the supposed working edge. The flint was thus not extensively reworked but likely dredged from primary context.

A greasy luster is visible on the surface of the flake. In addition, spots of a smooth, slightly domed and greasy polish are visible. The latter are only developed on the higher topography of the tool and are not necessarily connected to the edge. Immersing the lateral edge in a HCL and KOH solution did not remove the fatty sheen. The luster and the spots were interpreted as a form of post depositional surface modification, obscuring possible micro-wear traces. Along the supposed working edge a series of small retouches are present, some of which are recent. Compared to the original flake surface, the recent damage is dull in appearance and lacks post depositional modifications. Whether the older retouches are use-related or the result of fluviatile rolling or other natural processes is unclear. Unfortunately the greasy polish covering the flint surface makes it impossible to observe any wear traces. Use wear analysis with higher magnifications was therefore impossible and no conclusive traces of use were found.

X-ray micro-computed tomography (µ-CT)

The adhesive occupies a total volume of 1990 mm^3. It has been folded and pressed over the dorsal side of the flake and the dull lateral edge (Fig. 1A). The contact surface between the tar and the flake is estimated to be around 500 mm^2 and covers approximately one-quarter of the flint. The tar is no longer fully adhering to the flint surface, but is held in place as it is folded and locked around the edge of the flake. The tar has a rough rounded outer surface that protrudes 10.2 mm from the flake edge and shows a large concavity that has been possibly shaped with a finger. However, we have found no evidence for the presence of (partial) fingerprints (which are present on Königsaue piece A). The protrusion might be the remainder of a simple tar handle. The tar has a heterogeneous microstructure. Its outer surface consists of a layered coating 0.5 mm thick (Fig. 3A). The coating is tentatively attributed to weathering. Cracks that cross through the tar present similar signs of weathering. Thin veins of highly attenuating material run along the interface of the flint and the tar and penetrate the tar (Fig. 3B). Where the veins outcrop on the tar surface, it can be seen that they have an orange rust color. This combined with their high attenuation suggests that they consist of iron oxide. The veins may result from preferential weathering along cracks and ancient flow lines from when the tar was in a molten state during production. Some granular impurities follow the pattern of the iron oxide veins, while others are clustered. Visually, these resemble sand grains with a diameter of about 0.25 mm. However, their X-ray attenuation is higher than that of the flint silica and they could be iron oxide concretions. A few dark elongated inclusions appear on the scans, possibly charcoal fragments (Fig. 3C).

METHODS

^{14}C-AMS dating

We directly dated the adhesive to establish the age of the piece. Dating was performed at the Groningen laboratory, which has performed many dates on North Sea materials. AMS radiocarbon dating with AAA pretreatment (9) was selected as the most appropriate method in view of previous experience with North Sea materials.

THM-Pyrolysis-GC/MS

To confirm the hypothesis that the black material attached to the Zandmotor flake was birch tar, we used Thermally assisted Hydrolysis and Methylation Gas Chromatography Mass Spectrometry (THM-Py-GC/MS), with tetra methyl ammonium hydroxide (TMAH) for online hydrolysis and methylation. This is currently one of the best techniques to comprehensively characterize complex mixtures of organic compounds (19). By using pyrolysis as the sample introduction technique, the polymer fraction can also be analyzed.

Techno-typological analysis of the find and optical microscopy wear analysis

The flint flake was analyzed in techno-cultural terms, examining raw material and knapping characteristics, and was examined for post-depositional modifications. Optical microscopy was employed to determine the potential functioning of the flake. The flint flake was described following the guidelines developed for Middle Paleolithic artefacts from the Low Countries (18). The artefact was also studied using stereoscopic microscopy following the protocol established by (20).

X-ray micro-computed tomography (µ-CT)

We used X-ray micro-computed tomography (µ-CT) to analyze the internal structure of the adhesive and the morphology of the part of the flake obscured by the tar. µ-CT is a non-destructive technique (21) that can be used to inspect the internal composition and structure of a wide range of materials (22-25). We show how the adhesive was handled and applied by revealing the microstructure of the tar and exploring the interface between the flint and the tar. The surfaces of the flint and the tar were also modeled separately for interactive visualization and 3D printing (See (26) for the 3D file).

Supplementary Information Figures

Fig. S1. Map of western Eurasia with the find locations of chemically and spectrometrically identified and dated MP adhesives.

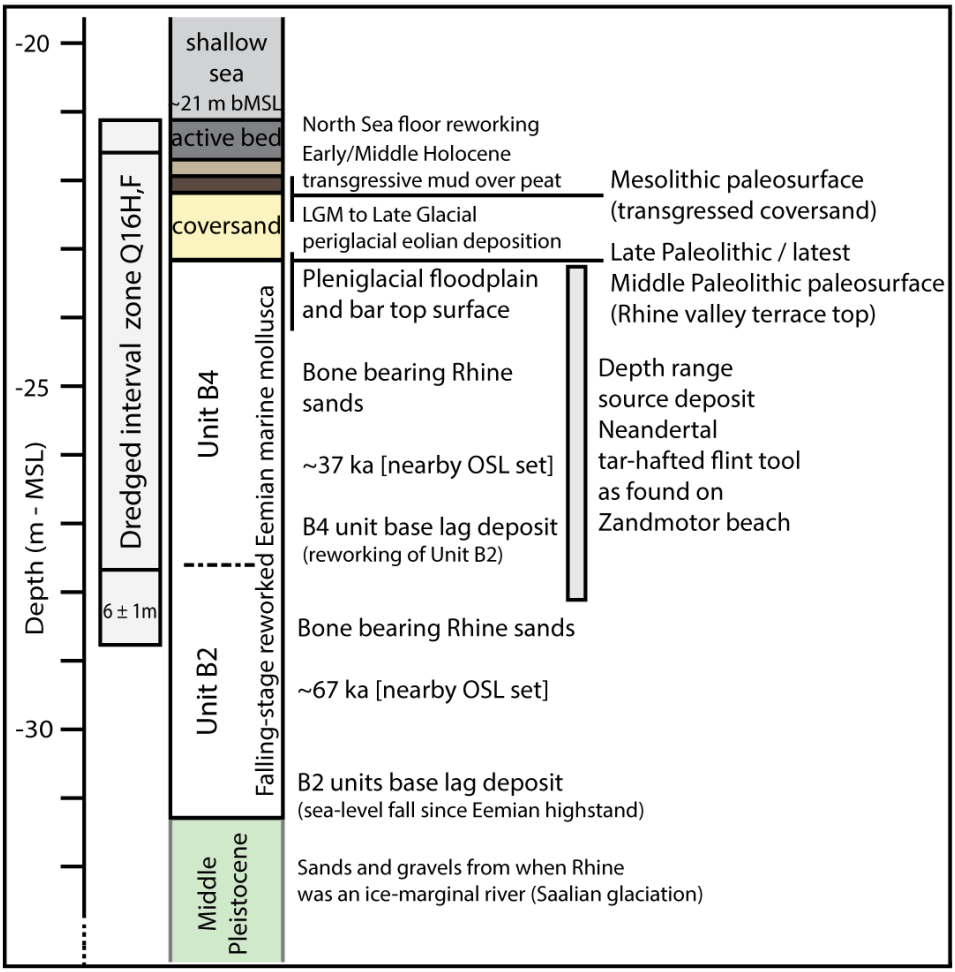

Fig. S2. Stratigraphy of the dredging area Q16. The upper 6-8 meters of the sedimentary column consist of: 1) a dynamic sheet of shelly sand of the active sea bed, 2) beds of Early-Middle Holocene transgressive tidal muds on basal peat, 3) Late Glacial eolian coversands containing Mesolithic materials (27, 28), and 4) medium to coarse grained fluvial sands of the Rhine-Meuse valley, Units B2 and B4, dating to 70-30 ka.

Fig. S3. Examples of Middle Paleolithic North Sea finds from the same geological context as the Zandmotor tar-backed find. A, B) Neandertal frontal bone from the Zeeland Ridges. C, D) Two handaxes from MV2. Images courtesy of the National Museum of Antiquities, the Netherlands (A, B, C), Frans de Vries/ToonBeeld and Remco Mouthaan (D).

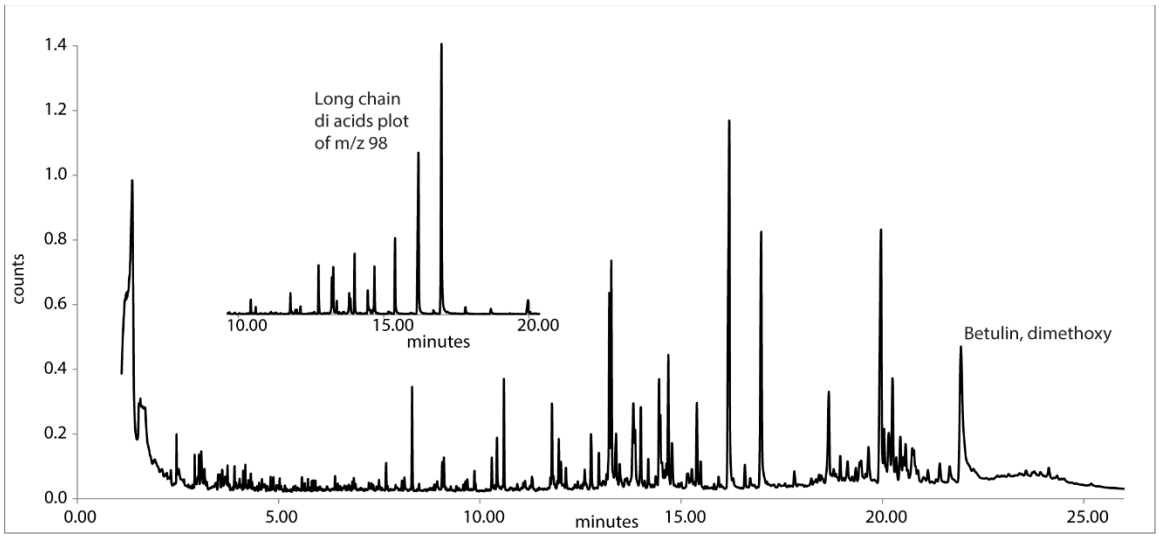

Fig. S4. THM-Py-GC/MS analysis of the black Zandmotor material, (dimethoxy) betulin is indicated. Insert shows presence of typical birch bark tar, long chain diacids (plot of m/z 98).

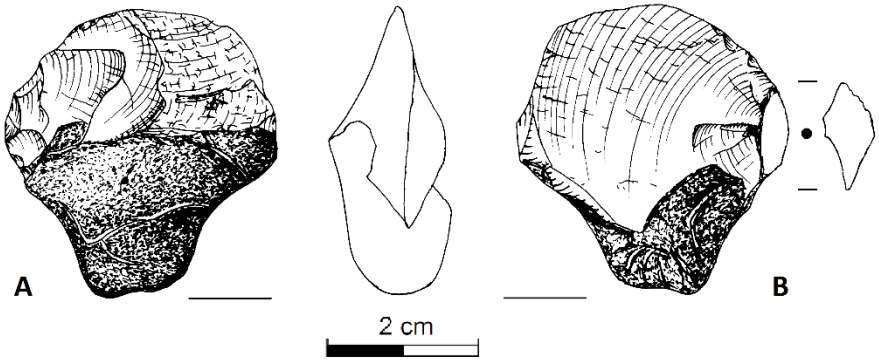

Fig. S5. Drawing of the Zandmotor flint flake with birch tar. A) dorsal side, B) ventral side. Closed circle: location of the point of percussion; short cross-hatching: natural frost-split face; stippling: birch tar (Drawing: Lykke Johansen, Archeological Drawings and Analyses).

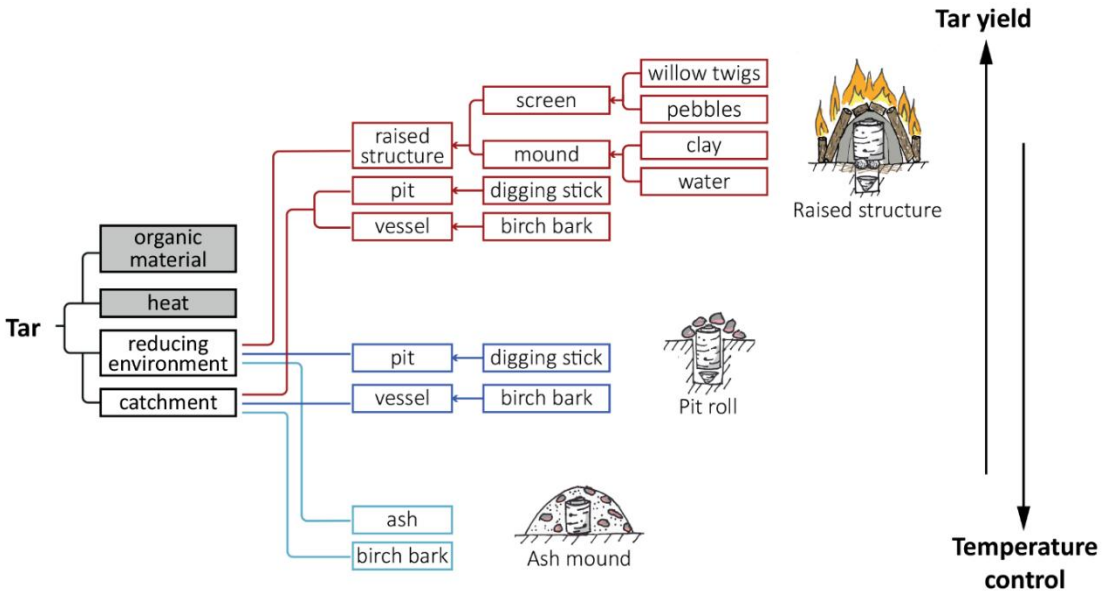

Fig. S6. Depiction of the increase in complexity of each tar production method and the associated increase in tar yield and decrease in required temperature control (Figure reprinted with permission from (29), Fig. 4, which is licensed under CC BY 4.0).

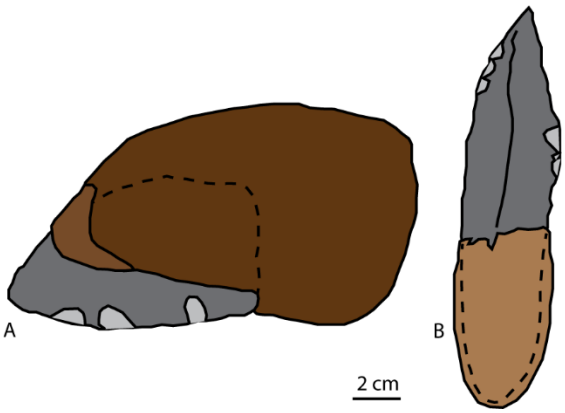

Fig. S7. Examples of adhesive backed/hafted tools. Dotted lines indicate the stone artifacts under the adhesives. A) Reconstruction of a stone tool hafted in the Königsaue *A* piece, light brown adhesives is what is preserved (after 30). B) Indigenous Leilira blade from Arnhem Land (after image 'Leilira blade' Australian Museum).

Supplementary Information Table

Table S1. The amount of time and energy required to collect firewood in a meadow, approximating the Late Pleistocene open woodland, and to produce the 1990 mm^3 of tar found at Zandmotor after (29, 31, 32).

	Tar production method			
	Simple *Condensation*	**Simple** *Ash mound*	**Intermediate** *Pit roll*	**Complex** *Raised structure*
Firewood required (kg):	-	84	60	43
Average time to collect firewood (min):	-	88	63	45
Average energy to collect firewood (kJ):	-	3283	2337	1673
Birch bark required (g):	959	234	94	24
Production/process time required (min)	613	545	148	56
Max tar yield (g tar/100 g bark)	0.22	0.97	2.42	9.63

References

1. F. S. Busschers *et al.*, Late Pleistocene evolution of the Rhine-Meuse system in the southern North Sea basin: imprints of climate change, sea-level oscillation and glacio-isostacy. *Quat. Sci. Rev.* **26**, 3216-3248 (2007).
2. B. Langeveld, De Zandmotor versus het strand van Hoek van Holland: opvallende verschillen in de vondstfrequentie van fossiele kleppen van bivalven geven informatie over de geologische geschiedenis van de zandwingebieden. *Afzettingen* **34**, 177-181 (2013).
3. F. S. Busschers *et al.*, Sedimentary architecture and optical dating of Middle and Late Pleistocene Rhine-Meuse deposits - fluvial response to climate change, sea-level fluctuation and glaciation. *Netherlands Journal of Geosciences - Geologie en Mijnbouw* **84**, 25-41 (2005).
4. T. Van Kolfschoten *et al.*, A remarkable collection of Late Pleistocene reindeer (Rangifer tarandus) remains from Woerden (The Netherlands). *Quat. Int.* **238**, 4-11 (2011).
5. M. P. Hijma, K. M. Cohen, W. Roebroeks, W. E. Westerhoff, F. S. Busschers, Pleistocene Rhine–Thames landscapes: Geological background for hominin occupation of the southern North Sea region. *Journal of Quaternary Science* **27**, 17-39 (2012).
6. S. N. Dudd, R. P. Evershed, Unusual triterpenoid fatty acyl ester components of archaeological birch bark tars. *Tetrahedron Letters* **40**, 359-362 (1999).
7. M. M. O'Connell, M. D. Bentley, C. S. Campbell, B. J. W. Cole, Betulin and lupeol in bark from four white-barked birches. *Phytochemistry* **27**, 2175-2176 (1988).
8. S. Orsini *et al.*, Micromorphological and chemical elucidation of the degradation mechanisms of birch bark archaeological artefacts. *Heritage Science* **3**, 1-11 (2015).
9. W. G. Mook, International comparison of proportional gas counters for 14 C activity measurements. *Radiocarbon* **25**, 475-484 (1983).
10. P. J. Reimer *et al.*, IntCal13 and Marine13 radiocarbon age calibration curves 0–50,000 Years cal BP. *Radiocarbon* **55**, 1869-1887 (2013).
11. H. Cheng *et al.*, Atmospheric 14C/12C changes during the last glacial period from Hulu Cave. *Science* **362**, 1293 (2018).
12. K. F. Helmens, The Last Interglacial–Glacial cycle (MIS 5–2) re-examined based on long proxy records from central and northern Europe. *Quaternary Science Reviews* **86**, 115-143 (2014).
13. E. T. H. Ran, Dynamics of vegetation and environment during the Middle Pleniglacial in the Dinkel Valley (The Netherlands). *Meded. Rijks Geol. Dienst*, 139-205 (1990).
14. T. Van der Hammen, G. C. Maarleveld, J. C. Vogel, W. H. Zagwijn, Stratigraphy, climatic succession and radiocarbon dating of the last glacial in the Netherlands. *Netherlands Journal of Geosciences - Geologie en Mijnbouw* **46**, 79-95 (1967).

15. W. H. Zagwijn, Vegetation, climate and radiocarbon datings in the Late Pleistocene of the Netherlands. Part II: Middle Weichselian. *Mededelingen Rijks Geologische Dienst, NS* **25**, 101-111 (1974).
16. C. J. Overweel, Distribution and transport of Fennoscandinavian indicators. A synthesis of data from the literature leading to a reconstruction of a pattern of flowlines and ice margins of the Scandinavian ice sheets. *Scripta Geologica* **43**, 1-117 (1977).
17. F. S. Busschers *et al.*, Response of the Rhine–Meuse fluvial system to Saalian ice-sheet dynamics. *Boreas* **37**, 377-398 (2008).
18. D. De Loecker, N. Schlanger, "Appendix 1. Analysing Middle Palaeolithic flint assemblages: The system used for studying the flint artefacts at Maastricht-Belvédère (The Netherlands)" in Analecta Praehistorica Leidensia 35/36/Beyond the Site: the Saalian archaeological record at Maastricht-Belvédère (the Netherlands), D. De Loecker, Ed. (Faculty of Archaeology, University of Leiden, Leiden, 2006), pp. 303-343.
19. H. Van Keulen, "The analysis and identification of transparent finishes using thermally assisted hydrolysis and methylation pyrolysis-gas chromatography-mass spectrometry" in Twelfth International Symposium on Wood and Furniture Conservation, M. Vasques Dias, Ed. (Stichting Ebenist, Amsterdam, 2014), pp. 134-141.
20. A. L. Van Gijn, The wear and tear of flint: Principles of functional analysis applied to Dutch Neolithic assemblages. *Analecta Praehistorica Leidensia* **22** (1990).
21. M. F. V. Tarplee, J. J. M. van der Meer, G. R. Davis, The 3D microscopic 'signature' of strain within glacial sediments revealed using X-ray computed microtomography. *Quat. Sci. Rev.* **30**, 3501-3532 (2011).
22. R. L. Abel *et al.*, Digital preservation and dissemination of ancient lithic technology with modern micro-CT. *Computers & Graphics* **35**, 878-884 (2011).
23. L. Bertrand *et al.*, Development and trends in synchrotron studies of ancient and historical materials. *Physics Reports* **519**, 51-96 (2012).
24. D. Ngan-Tillard, D. J. Huisman, "Micro-CT scanning" in Archaeological Soil and Sediment Micromorphology, C. Nicolsia, G. Stoops, Eds. (Wiley, 2017), pp. 441-449.
25. C. Tuniz, F. Zanini, "Microcomputerized Tomography (MicroCT) in Archaeology" in Encyclopedia of Global Archaeology, C. Smith, Ed. (Springer New York, New York, NY, 2014), 10.1007/978-1-4419-0465-2_675, pp. 4878-4884.
26. D. J. M. Ngan-Tillard *et al.*, X-ray micro-CT scan Data of First Middle Paleolithic tar backed tool from the Dutch North Sea. (4TU.Centre for Research Data, 2019). Dataset deposited 02/18/2019: https://doi.org/10.4121/uuid:0d7f284a-93ae-4d75-8361-984df49c2a4e.
27. Amkreutz, L., et al., *Meer dan bijvangst! De prehistorische archeologie van de Noordzee.* Cranium, 2017. **34**(1): p. 34-47.
28. Van der Plicht, J., et al., *Surf'n Turf in Doggerland: Dating, stable isotopes and diet of Mesolithic human remains from the southern North Sea.* Journal of Archaeological Science: Reports, 2016. **10**: p. 110-118.

29. P. R. B. Kozowyk, M. Soressi, D. Pomstra, G. H. J. Langejans, Experimental methods for the Palaeolithic dry distillation of birch bark: Implications for the origin and development of Neandertal adhesive technology. *Sci. Rep.* **7**, 8033 (2017).
30. H. Mellar, *Kataloge zur Dauerausstellung im Landesmuseum für Vorgeschichte Halle: Paläolithikum und Mesolithikum*, Begleithefte zur Dauerausstellung im Landesmuseum für Vorgeschichte Halle (Landesmuseum für Vorgeschichte, Halle, 2004).
31. A. G. Henry, T. Büdel, P.-L. Bazin, Towards an understanding of the costs of fire. *Quaternary International* **493**, 96-105 (2018).
32. P. Schmidt *et al.*, Birch tar production does not prove Neanderthal behavioral complexity. *Proceedings of the National Academy of Sciences* 10.1073/pnas.1911137116, 201911137 (2019).